

Estimation of Forearm Pose Based on Upper Arm Deformation Using a Deep Neural Network

Sung-Gwi Cho¹, Tetsuya Kurasumi¹, Masahiro Yoshikawa²,
Ming Ding^{1,3}, Jun Takamatsu¹, and Tsukasa Ogasawara¹

Abstract—Activities of body tissues such as muscles, tendons, and bones appear in the deformation of skins. It would be possible to obtain the information of the body motions by measuring the skin deformation. In our research, we focused on upper arm deformation, which is changed with not only the elbow flexion and extension but also the forearm pronation and supination. Thus, with the measurement of the upper arm deformation, we can estimate the elbow pose. In this paper, we propose a forearm pose estimation method based on upper arm deformation. A distance sensor array with eight sensor units is developed to measure the upper arm deformation. From the measured deformation, a deep neural network (DNN) based model is trained and used to estimate the forearm pose. The results of experiment show that our proposed method was able to estimate the forearm pose with RMSE of 2.9 degrees for the elbow joint angle and 7.6 degrees for the forearm pronation and supination angle.

I. INTRODUCTION

Bio-signals could provide the activities of the body tissues related to the human motions. Such signals can be measured by many kinds of wearable sensors. Human motion estimation/analysis based on bio-signals have gained popularity. Bio-signals have used in many areas, such as intuitive operation for robotic/computer devices [1]–[3], analysis of the motions in the medical, welfare, sporting fields [4], [5].

In our daily life, the motion of upper limbs plays a very important role for grasping and manipulating the daily use objects. To estimate the motions, various types of the bio-signals have been used. The typical one is the sEMG [6], [7], which can provide the activities of the muscles related to upper limb motions. Various mechanical information have also been used for motion estimation such as the force distribution between the fixture and human surface [8]–[10] and the bend information on the forearm [11].

In our research, we focused on a deformation of the skin [12], [13], a type of bio-signals which provides activities of not only the muscles but also the tendons and bones. In our previous study, we measured the forearm deformation and was able to use it to estimate the joint angles of the hand [14].

¹S.-G. Cho, T. Kurasumi, M. Ding, J. Takamatsu, and T. Ogasawara are with the Division of Information Science, Nara Institute of Science and Technology (NAIST), Japan (cho.sungi.cg3, kurasumi.tetsuya.kj4, ding, j-taka, ogasawara)@is.naist.jp

²M. Yoshikawa is with Faculty of Robotics & Design Engineering, Osaka Institute of Technology (OIT), Japan masahiro.yoshikawa@oit.ac.jp

³M. Ding is also with Institutes of Innovation for Future Society, Nagoya University, Japan

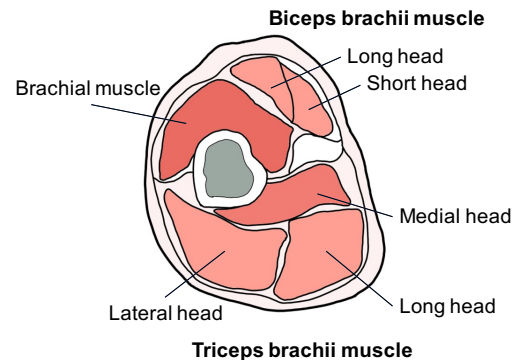


Fig. 1. Cross-section of the upper arm

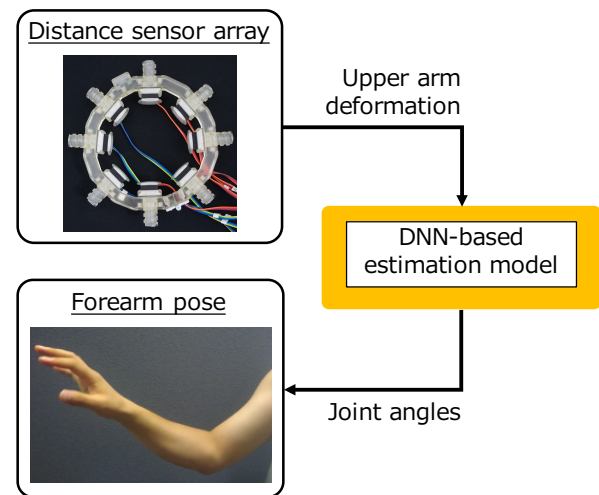


Fig. 2. Overview of the proposed method

Upper arm deformation also has rich information of the upper limb motions. As shown in Fig. 1, there are three major muscles in the upper arm, the biceps brachii, triceps brachii, and brachial muscles. Upper arm deformation would happen not only when the elbow is flexed and extended but also when the forearm is pronated and supinated because the biceps brachii muscle also works to supinate the forearm. Upper arm deformation provides not only elbow motion but also forearm pronation and supination motion.

In this paper, we propose a new method to estimate the pose of the forearm (flexion/extension, pronation/supination) based on the upper arm deformation. To estimate the forearm

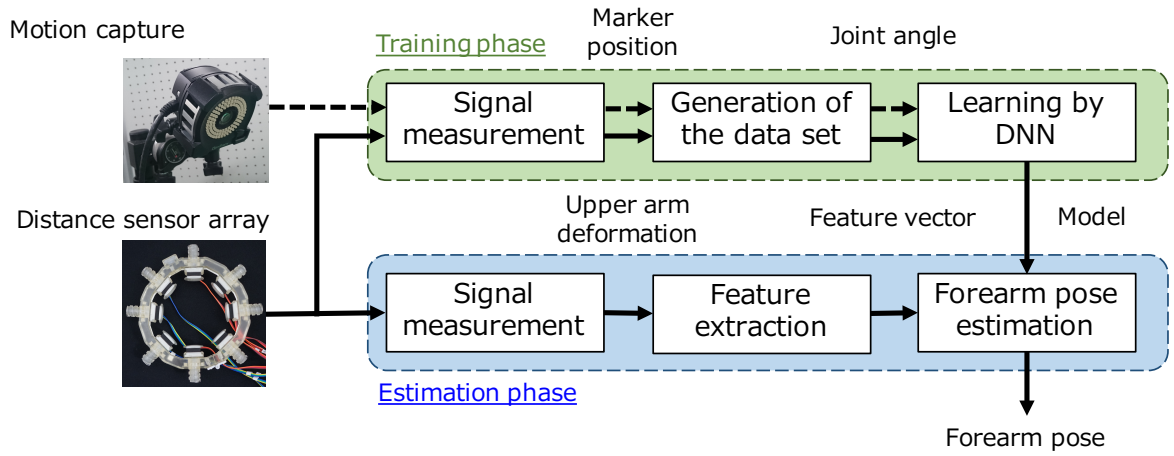


Fig. 3. Procedure of the proposed method

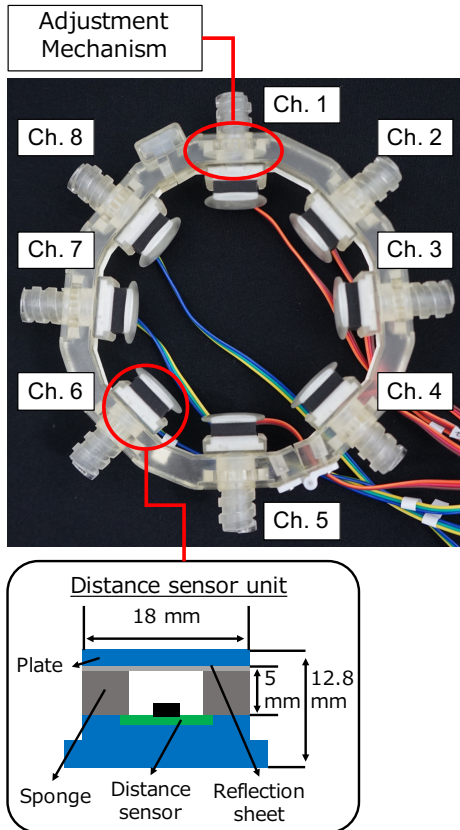


Fig. 4. Structure of the distance sensor array

pose using the *upper-arm* deformation, it removes the limitation on input measurement positions in various applications. As shown in Fig. 2, first, we measure upper arm deformation using a distance sensor array which is developed to measure the deformation for various users. Second, we train a deep neural network (DNN) based model [15] that estimates the elbow joint angle and the forearm pronation and supination angle. Finally, in a motion estimation experiment, we evalu-

ate the performance of the proposed method with combined motions of the elbow flexion and extension and the forearm pronation and supination.

Contributions of this paper are as follows: First, we proposed a forearm pose estimation method based on only upper arm deformation. Second, we developed a distance sensor array to fit the upper arms for various users. We design the sensor arrangement to enclose the whole circumference of an upper arm, while using as many sensors as possible sensor units to measure deformation in detail; that is useful to measure the small difference in pronation and supination.

II. METHOD

A. Method overview

As shown in Fig. 3, the proposed method consists of three parts: signal measurement, generation of the data set including feature extraction, and motion estimation by a DNN-based model.

(1) Signal measurement

In this part, we measure the signals of the upper arm deformation using the developed sensor array. In the training phase, as the target value of the forearm pose, we also set some markers on the body and measure the positions of them by using a motion capture device.

(2) Generation of the data set

To train the machine learning based method, in this part, we extract feature vectors from the measured data of the distance sensor array. The target values of the forearm poses is calculated from the positions of the markers. By synchronizing the feature vectors and the forearm poses, the data pairs can be created.

(3) Learning & estimation by DNN

The pairs of extracted feature vectors and calculated forearm poses train the DNN-based estimation model. Using the trained model, the forearm pose

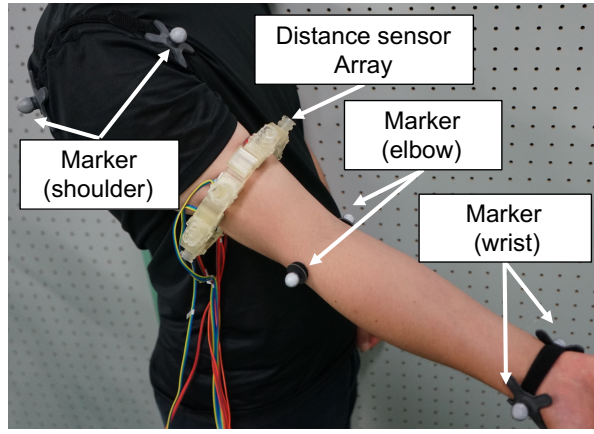


Fig. 5. Measurement setup

can be estimated from the feature vector of the upper arm deformation.

In the training phase, using measured upper arm deformation from the distance sensor array and forearm poses, the DNN-based model is trained to estimate elbow poses. In the estimation phase, when upper arm deformation is inputted, the method estimates forearm poses by using the trained model.

B. Signal measurement

For measuring the upper arm deformation, a distance sensor array is developed, as shown in Fig. 4. This array can measure the whole circumference of upper arm deformation using eight of distance sensor units. The sensor unit converts a distance between a distance sensor and a plate to a voltage. More detailed explanation of the distance sensor unit has been described in our previous paper [14]. We design the shape of the sensor array to fit the upper arm to arrange Ch. 1 and Ch. 5 on the biceps brachii and the triceps brachii muscles. An adjusting mechanism has also been designed to fit the size of the array for various size of the upper arm. We attach the developed distance sensor array to the user's upper arm by setting the Ch. 1 sensor unit on the biceps brachii muscle, as shown in Fig 5.

In the training phase, we also measure the forearm poses using a motion capture, as shown in Fig. 5. Every two markers of the motion capture are also attached on the shoulder, the elbow, and the wrist.

The distance sensor array, A/D converter, stable power source are connected with cables. The A/D converter and a PC is connected with a USB cable. A Motion capture system and the PC are connected with a LAN cable. The upper arm deformation could be measured at 1200Hz. Data of the motion capture is measured at 120Hz.

C. Generation of the data set

To train the estimation model, we need to make a training data set of upper arm deformation and the forearm pose.

The measured data of the distance sensor array are synchronized to match these frame rates at 120 Hz, which is the

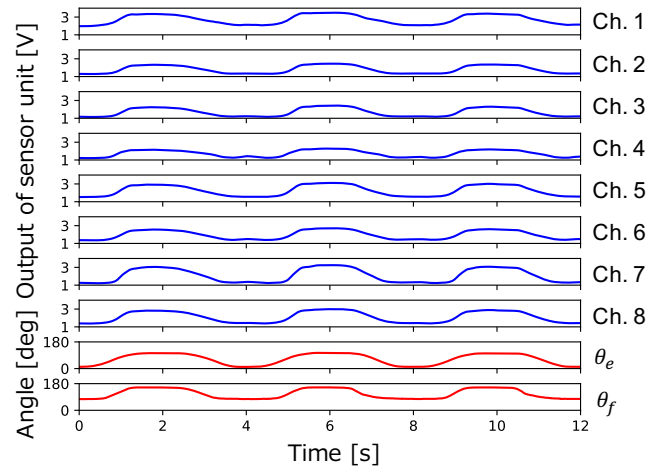


Fig. 6. An example of the feature vector and the forearm pose

same as the measured data of the motion capture device. The feature vector (\mathbf{x}) is defined by the average of every $N = 10$ samples as follows:

$$APR_l(p) = \frac{1}{N} \sum_{n=1}^N PR_l(n), \quad (1)$$

where $PR_l(n = 1, \dots, N; l = 1, \dots, L)$ is the n_{th} sampled signal measured with the l_{th} channel in the p_{th} frame. In this study, eight sensor units are used in the sensor array, that is $L = 8$. The feature vector $\mathbf{x}(p)$ consists of the L -dimensional APR as follows:

$$\mathbf{x}(p) = (APR_1(p), \dots, APR_L(p)). \quad (2)$$

In the estimation phase, we also use this extracted feature vector.

We also calculate the elbow and the wrist coordinate from the position of each two joint markers and these middle point. The elbow joint angle (θ_e) and the forearm pronation and supination angle (θ_f) are calculated from the elbow and the wrist coordinate. The target value $\mathbf{y}(p)$ consists of θ_e, θ_f as follows:

$$\mathbf{y}(p) = (\theta_e(p), \theta_f(p)). \quad (3)$$

Fig. 6 shows an example of the extracted feature vectors and the forearm poses (θ_e and θ_f) when a user moves the forearm pose of neutral to pronation during the elbow flexion and extension. We can find that the deformation on each sensor unit could be measured with the changing of the forearm pose.

D. Learning & estimation by DNN

Using the feature vector \mathbf{x} and the target value \mathbf{y} , a DNN-based model is trained to estimate the forearm pose. The model simultaneously estimates two types of joint angles (θ_e and θ_f) at the same time.

Fig. 7 shows the architecture of the proposed model. A fully-connected multiple layer neural network model is used.

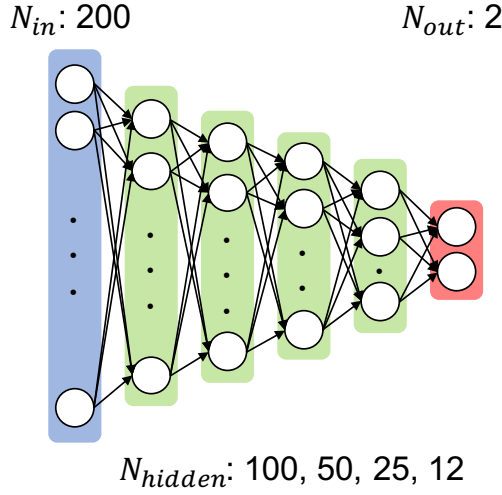


Fig. 7. Architecture of the model

The proposed model consists of input and output layer and four hidden layers. To consider a time series of the upper arm deformation, the input of the model is Z frames feature vector. In this method, $Z = 25$ frames data (0.1 seconds (12 frames) in before and after the target frames) is used as the input data. The number of the input nodes N_{in} is $L \times Z = 200$. The output N_{out} is two joint angles θ_e and θ_f . Number of the nodes of each hidden layer (N_{hidden}) are 100, 50, 25, 12. A ReLu is used for the activation function for each layer.

Adam [16] is used as the optimization function, and the mean squared is used as the loss function. The model is trained with a batch size of 128 and 150 epochs.

III. EXPERIMENT

To confirm the performance of the proposed method, we performed a forearm pose estimation experiment. The experimental protocol of this study was approved by the research ethics board of Nara Institute of Science and Technology. Before participation in the experiment, the informed consent was obtained from the subjects.

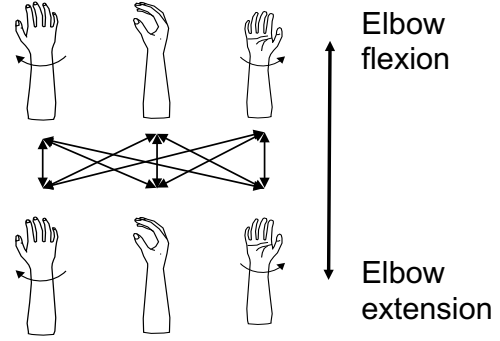
A. Conditions

We performed the experiment with five healthy subjects (the 20's, male, right-handed). The subjects wore the distance sensor array and motion capture marker and performed different motion: the elbow flexion and extension, and the pronation and supination of the forearm simultaneously. In this experiment, we asked the subjects to move their forearm with fixing the upper arm pose.

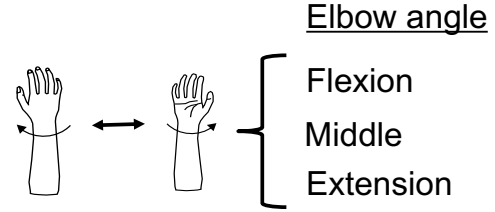
For each subject, 12 repetitions of motions were measured in each of the following two conditions:

Condition 1

Subjects move their forearm to three poses (pronation, neutral, and supination) when flexing and extending the elbow joint, as shown in Fig. 8(a). In one trial, the elbow flexion and extension were



(a) condition 1



(b) condition 2

Fig. 8. Measured motion condition

performed three times. Nine types of movements were performed by every subject.

Condition 2

Subjects move their forearm from pronation to supination with a fixed elbow joint angle (flexion, middle, and extension), as shown in Fig. 8(b). In one trial, the forearm pronation and supination were performed three times. Three types of movements were performed by the subjects.

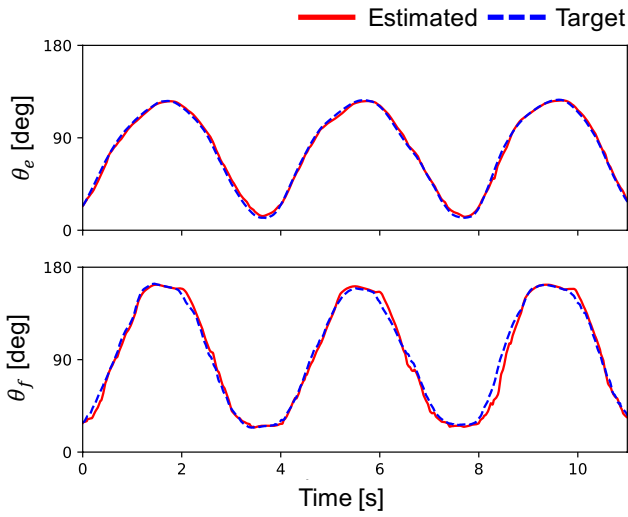
One trial was taken 12 seconds. Subjects performed every movement 5 times. The total number of the trials was $12 \times 5 = 60$.

For the evaluation, we tested 60 trials data with five-fold cross-validation. Every four trials data of each pattern were used for training and the remaining one trial data of each pattern were used for testing. The number of one trial data was 1416. Thus, the number of the training data was 67968 and the number of the testing data was 16992. The pose estimation model was trained with each subject.

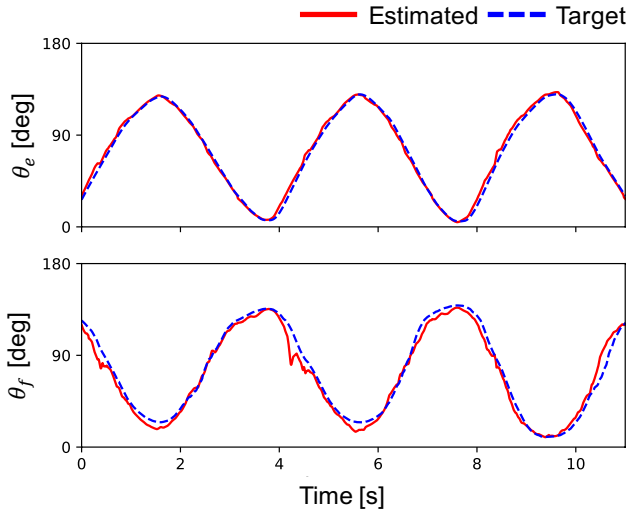
The performance of the proposed method was evaluated with the root mean squared error (RMSE). The RMSE of each joint angle was calculated as follows:

$$\text{RMSE} = \sqrt{\frac{1}{M} \sum_{m=1}^M (\theta_{\text{Target}}(m) - \theta_{\text{Estimated}}(m))^2}, \quad (4)$$

where M is the total number of frames for the testing data, θ_{Target} is the joint angles acquired from the motion capture, and $\theta_{\text{Estimated}}$ is the estimated joint angles using the proposed method in the m_{th} frame.

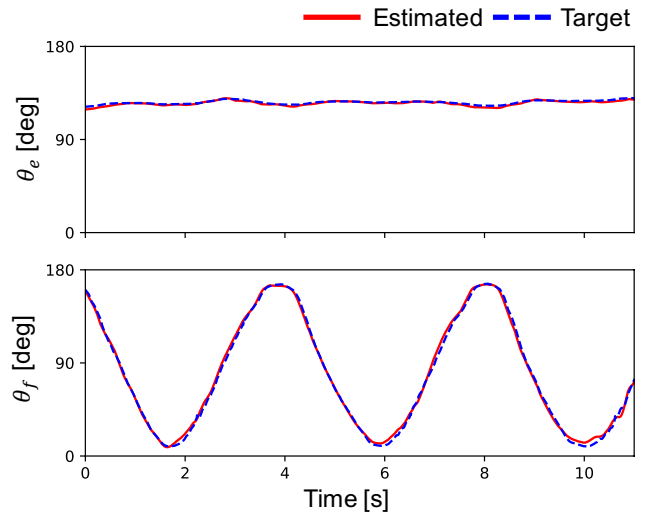


(a) Supination to Pronation

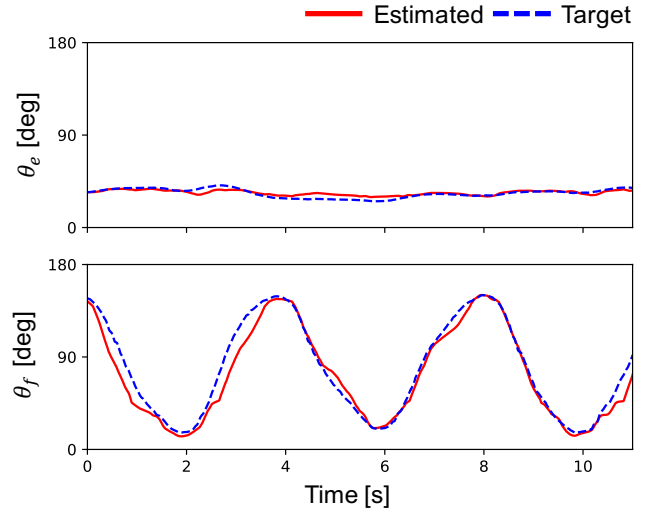


(b) Pronation to Supination

Fig. 9. Estimation results on the condition 1



(a) Flexion



(b) Extension

Fig. 10. Estimation results on the condition 2

B. Results

Fig. 9 and Fig. 10 shows an example of the estimation result for subject A in both motion conditions.

Fig. 9 shows the estimated results when the subject moved the forearm between supination/pronation to pronation/supination during the elbow flexion and extension in condition 1. The red line shows the estimated joint angles and the blue broken line shows the target joint angles. In condition 1, the estimated joint angles were matched to the target joint angles in both joints.

Fig. 10 shows the estimated results when the subject pronated and supinated the forearm when fixing the elbow joint angle in condition 2. In condition 2, the estimated joint angles were also matched to the target joint angles well in both joints.

In both conditions, the method was able to estimate the two joint angles of the forearm pose. There was no large

difference between the estimated pose and the target pose and no large phase difference. Table I shows RMSE of each subject and the average of all subjects. The average RMSEs of all subjects were 2.9 degrees for the θ_e , and 7.6 degrees for the θ_f . The maximum RMSEs of the joint angles were 3.9 degrees for the θ_e , and 10.1 degrees for the θ_f .

IV. DISCUSSION

The RMSE of the elbow joint angle (θ_e) was lower than that of the forearm pronation and supination angle (θ_f). This is because the muscles in the upper arm such as the biceps brachii and the triceps brachii muscles mainly contribute to the elbow flexion and extension. These muscles contribute to the forearm pronation and supination on a certain level, though the other muscles mainly work for these motions. It may be the reason that the RMSE of the θ_f is also not large.

In condition 2, when comparing the estimation results of the θ_f between the flexion and extension of the elbow pose,

TABLE I
RMSE FOR EACH SUBJECT

	θ_e [deg]	θ_f [deg]
A	2.4	6.4
B	2.5	7.8
C	2.5	6.8
D	3.2	6.3
E	3.9	10.1
Ave.	2.9	7.6

results of the flexion was better, as shown in Fig. 10. It is because the biceps brachii muscle also works to supinate when the elbow joint was flexed. Since there were no large difference between the estimated and the target θ_f when the elbow joint was extended, the estimation was possible if the activities of biceps brachii were small.

These results showed that the forearm poses were able to estimate based on only upper arm deformation using our proposed method.

V. CONCLUSION

In this study, we proposed a forearm pose estimation method based on upper arm deformation. First, we measured upper arm deformation using our developed distance sensor array. A fully-connected 6-layer deep neural network model was created to estimate the joint angles from the measured deformation. In the motion estimation experiment, we verified the performance of the proposed method with combined motions of flexion and extension of the elbow and pronation and supination of the forearm. The average of RMSE for five subjects was 2.9 degrees for the θ_e , and 7.6 degrees for the θ_f . The results showed that our proposed method was able to estimate the forearm poses at the joint angle level. In the future, to verify the performance of the method more carefully, we will try to increase number of the subjects. We will also verify the performance of the method in random motion patterns and different motion speeds.

ACKNOWLEDGMENT

This research was and Tateisi Science and Technology Foundation (grant number 2187007).

REFERENCES

[1] A. Atasoy, E. Kaya, E. Toptas, S. Kuchimov, E. Kaplanoglu, and M. Ozkan, "24 dof EMG controlled hybrid actuated prosthetic hand," in *Proceedings of the 2016 38th Annual International Conference of the IEEE Engineering in Medicine and Biology Society (EMBC)*, pp. 5059–5062, 2016.

[2] C. Meeker, S. Park, L. Bishop, J. Stein, and M. Ciocarlie, "EMG pattern classification to control a hand orthosis for functional grasp assistance after stroke," in *Proceedings of the 2017 international conference on rehabilitation robotics (ICORR)*, pp. 1203–1210, 2017.

[3] Y. Yun, S. Dancausse, P. Esmatloo, A. Serrato, C. A. Merring, P. Agarwal, and A. D. Deshpande, "Maestro: an EMG-driven assistive hand exoskeleton for spinal cord injury patients," in *Proceedings of the 2017 IEEE International Conference on Robotics and Automation (ICRA)*, pp. 2904–2910, 2017.

[4] B. Ploderer, J. Fong, A. Withana, M. Klaic, S. Nair, V. Crocher, F. Vetere, and S. Nanayakkara, "Armsleeve: a patient monitoring system to support occupational therapists in stroke rehabilitation," in *Proceedings of the 2016 ACM Conference on Designing Interactive Systems*, pp. 700–711, 2016.

[5] S. Fantozzi, A. Giovanardi, F. A. Magalhães, R. Di Michele, M. Cortesi, and G. Gatta, "Assessment of three-dimensional joint kinematics of the upper limb during simulated swimming using wearable inertial-magnetic measurement units," *Journal of Sports Sciences*, vol. 34, no. 11, pp. 1073–1080, 2016.

[6] L. Pan, D. L. Crouch, and H. H. Huang, "Comparing EMG-based human-machine interfaces for estimating continuous, coordinated movements," *IEEE Transactions on Neural Systems and Rehabilitation Engineering*, 2019.

[7] F. Xiao, Y. Wang, L. He, H. Wang, W. Li, and Z. Liu, "Motion estimation from surface electromyogram using adaboost regression and average feature values," *IEEE Access*, vol. 7, pp. 13 121–13 134, 2019.

[8] Z. G. Xiao and C. Menon, "Performance of forearm FMG and sEMG for estimating elbow, forearm and wrist positions," *Journal of Bionic Engineering*, vol. 14, no. 2, pp. 284–295, 2017.

[9] N. Li, S. Wei, M. Wei, B. Liu, H. Huo, and L. Jiang, "Hand motion recognition based on pressure distribution maps and ls-svm," in *Proceedings of 2014 International Conference on Mechatronics and Control (ICMC)*, pp. 1027–1031, 2014.

[10] P.-G. Jung, G. Lim, S. Kim, and K. Kong, "A wearable gesture recognition device for detecting muscular activities based on air-pressure sensors," *IEEE Transactions on Industrial Informatics*, vol. 11, no. 2, pp. 485–494, 2015.

[11] Y. Kamei and S. Okada, "Classification of forearm and finger motions using electromyogram and arm-shape-changes," in *Proceedings of 2016 38th Annual International Conference of the IEEE Engineering in Medicine and Biology Society (EMBC)*, pp. 5680–5683, 2016.

[12] A. Kato, Y. Matsumoto, R. Kato, Y. Kobayashi, H. Yokoi, M. G. Fujie, and S. Sugano, "Estimating wrist joint angle with limited skin deformation information," *Journal of Biomechanical Science and Engineering*, vol. 13, no. 2, pp. 1–11, 2018.

[13] R. Fukui, M. Watanabe, M. Shimosaka, and T. Sato, "Hand-shape classification with a wrist contour sensor: Analyses of feature types, resemblance between subjects, and data variation with pronation angle," *The International Journal of Robotics Research*, vol. 33, no. 4, pp. 658–671, 2014.

[14] S.-G. Cho, M. Yoshikawa, M. Ding, J. Takamatsu, and T. Ogasawara, "Estimation of hand motion based on forearm deformation," in *Proceedings of 2018 IEEE International Conference on Robotics and Biomimetics (ROBIO)*, pp. 2291–2296, 2018.

[15] Y. Bengio *et al.*, "Learning deep architectures for AI," *Foundations and trends® in Machine Learning*, vol. 2, no. 1, pp. 1–127, 2009.

[16] D. P. Kingma and J. Ba, "Adam: A method for stochastic optimization," *arXiv preprint arXiv:1412.6980*, 2014.